GPS Solut
DOI 10.1007/s10291-014-0387-3

ORIGINAL ARTICLE

# Topo-Iberia project: CGPS crustal velocity field in the Iberian Peninsula and Morocco

**J. Garate · J. Martin-Davila · G. Khazaradze · A. Echeverria · E. Asensio · A. J. Gil · M. C. de Lacy · J. A. Armenteros · A. M. Ruiz · J. Gallastegui · F. Alvarez-Lobato · C. Ayala · G. Rodríguez-Caderot · J. Galindo-Zaldívar · A. Rimi · M. Harnafi**

Received: 7 April 2014 / Accepted: 29 May 2014


**Abstract** A new continuous GPS network was installed under the umbrella of a research project called "Geociencias en Iberia: Estudios integrados de topografía y evolución 4D (Topo-Iberia)", to improve understanding of kinematic behavior of the Iberian Peninsula region. Here we present a velocity field based on the analysis of the 4 years of data from 25 stations constituting the network, which were analyzed by three different analysis groups contributing to the project. Different geodetic software packages (GIPSY–OASIS, Bernese and GAMIT) as well as different approaches were used to estimate rates of present day crustal deformation in the Iberian Peninsula and Morocco. In order to ensure the consistency of the velocity fields determined by the three groups, the velocities obtained by each analysis center were transformed into a common Eurasia Reference Frame. After that, the strain rate field was calculated. The results put in evidence more prominent residual motions in Morocco and southernmost part of the Iberian Peninsula. In particular, the dilatation and shear strain rates reach their maximum values in the Central Betics and northern Alboran Sea. A small region of high shear strain rate is observed in the east-central part of the peninsula and another deformation focus is located around the Strait of Gibraltar and the Gulf of Cadiz.

**Keywords** CGPS networks · Iberia Morocco region · Tectonic motion

## Introduction

The Iberian Peninsula and its continental margins is the area of the research initiative known as Topo-Iberia,

**Electronic supplementary material** The online version of this article (doi:10.1007/s10291-014-0387-3) contains supplementary material, which is available to authorized users.

J. Garate (✉) · J. Martin-Davila
Real Instituto Observatorio Armada, 11100 San Fernando, Cádiz, Spain
e-mail: jgarate@roa.es

G. Khazaradze · A. Echeverria · E. Asensio
Dpto. Geodinámica i Geofísica, University of Barcelona, Barcelona, Spain

A. J. Gil · M. C. de Lacy · J. A. Armenteros · A. M. Ruiz
Dpto. Ing. Cartográfica, Geodesia y Fotogrametría, University of Jaen, Jaén, Spain

A. J. Gil · M. C. de Lacy · J. A. Armenteros · A. M. Ruiz
CEACTierra. Centro de EstudiosAvanzados de Ciencias de la Tierra, Jaén, Spain

J. Gallastegui
Dpto. Geología, University of Oviedo, Oviedo, Spain

F. Alvarez-Lobato
Dpto. Geología, University of Salamanca, Salamanca, Spain

C. Ayala
Instituto Geológico Minero de España, Madrid, Spain

C. Ayala
Institute of Earth Sciences Jaume Almera-CSIC, Barcelona, Spain

G. Rodríguez-Caderot
Dpto. Astronomía y Geodesia, Complutense University of Madrid, Madrid, Spain

J. Galindo-Zaldívar
Dpto. Geodinámica, Universidad de Granada, Granada, Spain

A. Rimi · M. Harnafi
Institute Scientifique, University Mohammed V-Agdal, Rabat, Morocco

Published online: 21 June 2014

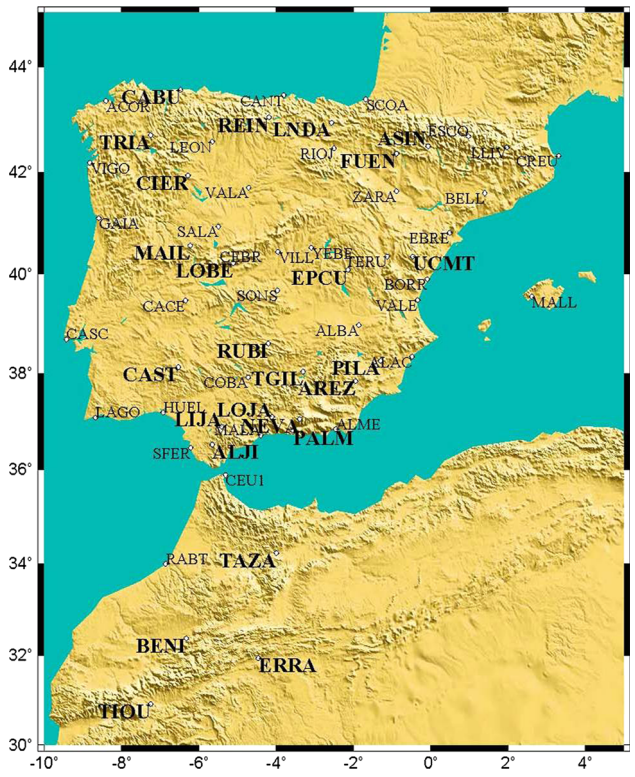


**Fig. 1** The Iberian Region, extended to Morocco to include the Atlas Mountains Range. Topo-Iberia CGPS Network and EUREF/IGS CGPS stations in the region are shown. Positions for the Topo-Iberia stations are included in Table SM1 (Supplementary Material)

funded by the Spanish Government through the Research project CSD2006-00041, named *Geociencias en Iberia: Estudios integrados de topografía y evolución 4D* ("*Topo-Iberia*"). Developing and exploiting a new integrated database including geologic, seismic, geodetic and magnetotelluric observations, the project will produce a complete overview of interactions among deep, shallow and surface processes like tectonics, mass transport and landscape evolution.

The primary geodetic contribution to the project is a new CGPS network implementation, avoiding if possible to setup antennae on buildings in populated areas. Twenty-six new stations were located, including four in Morocco. To optimize the network configuration, already existing public GPS networks located in the region were used. Figure 1 shows the new network and the additional CGPS used to derive the regional deformational behavior.

Data analysis was made by three different groups, using different software packages and different approaches. Results were combined after a previous comparison which shows very good agreement among the solutions. Comparisons of different solutions were carried out by some authors before now. Dietrich et al. (2001) analyzed planimetric and altimetric components, Kierulf et al. (2008) studied the vertical components and Avallone et al. (2010) compared horizontal components. Individual results as well as combined results among different solutions are presented in the manner similar to Kierulf et al. (2008).

Individual solutions were aligned to the International Terrestrial Reference Frame (ITRF) to build time series producing velocity values for the points. But some gaps occurred in some stations, for different reasons: at the beginning of 2009, faults in the antennas were detected at some sites. Antennae replacements produced jumps in the series, which values have to be calculated. Anyway, time series analysis was carefully performed. Furthermore, several sites suffered vandalism attacks, for example stations REIN and VILA. While the former could be repaired, the latter had to be dismantled. This is the reason why the results of VILA are not included.

To compile more complete information about the behavior of the region, the previously ITRF aligned points were subsequently transformed to the European Reference Frame (ETRF), as defined by the European Permanent Network (Bruyninx et al. 2009). Small deformations are easier to detect and to interpret in the regional frame.

The whole analyzed network consists of about 60 CGPS stations, although the network analysis approaches use more than 100 CGPS to connect their solutions to the ITRF. Continuous GPS stations operated by different institutions: IGS (http://igscb.jpl.nasa.gov), EUREF (http://www.epncb.oma.be) and other Spanish governmental as well as regional offices and CGPS data files from private companies were used along with the 26 CGPS stations strategically built for the Topo-Iberia project. The regional network we are showing includes data from all of these receivers. Since the new network was fully operational at the end of 2008, the processed time series include 4 years of continuous data, long enough time span to produce statistically significant results and to avoid problems of correlated parameters as suggested by Blewitt and Lavallée (2002).

## GNSS data processing

Data analysis was performed by three different groups, with different approaches. Each group used one of the best-known geodetic analysis software packages. Precise point positioning (PPP) approach with GIPSY–OASIS (Zumberge et al. 1997), developed at Jet Propulsion Laboratory (JPL) was used at San Fernando Naval Observatory (ROA). Geodetic network approach was used by the University of Jaen (UJA) group using Bernesse software (Dach et al. 2007) and also by the University of Barcelona (UB) group by using GAMIT (Herring et al. 2008), software developed at the Massachusetts Institute of Technology.

### Analysis at ROA using GIPSY–OASIS software

The Precise point positioning (PPP) approach implemented in the GIPSY–OASIS software takes advantage of the large quantity of GPS stations observing the same set of satellites everyday throughout the world. In such a way, the JPL analysis center determines precise satellite positions and clock corrections from a globally distributed GPS receiver network. Daily files including satellite clock corrections and yaw angles are issued at the JPL FTP server together with satellite orbits and earth orientation parameter information. Since all the data we use are calculated in an unconstrained, so-called free-network, transformation parameters to an ITRF realization must also be included. Once this orbital information is issued, data files from the local network are analyzed by estimating their own receiver parameters with their collected data, using those satellite parameters included in the downloaded files. Each site atmospheric zenith delay and receiver clock biases were estimated. Absolute antennae phase center variation was included into the analysis by using the antex files issued by the International GNSS Service, for the corresponding ITRF realization. We used the GOT00.2_PP model for the ocean-loading coefficients, calculated at the Onsala Space Observatory (Scherneck 1991). Since the beginning of April 2009, JPL has also produced new parameter files with information about widelanes and smoothed estimated phase biases from each GPS satellite to each one of the GPS receivers included in the above-mentioned globally distributed network. These files will allow GIPSY software final users to derive ambiguity solutions for single receiver data files analysis. The final step is to align the calculated ambiguity fix solution to the ITRF applying the seven parameter transformation downloaded from the JPL server. Formal errors are independent of the network from which global parameters were derived (Zumberge et al. 1997). Characteristics of processing with GIPSY–OASIS are summarized in Table SM2 included in the supplementary material.

The greatest advantage of this approach is how fast the analysis is, as it does not need to combine baselines for the different stations included in the solution. It takes less than 1 min to analyze a daily file for one station. Furthermore, if a new station has to be included in the solution after a first analysis, it is not necessary to repeat the whole network or subnetwork calculation and adjustment. Also, errors in the analysis of the files of a station data do not contaminate the results for the neighbor stations analyzed.

Stacking daily position solutions produces time series for each of the site coordinates. As a first approximation, linear trends derived from coordinate time series generate velocities in the corresponding direction. But seasonal effects and eventual jumps in the series must be taken into account to obtain more accurate results. Furthermore, formal errors obtained from the raw time series are too optimistic, as they are treated only as white noise. A combination of white and flicker noise is more appropriate for most of the sites (Johnson and Agnew 1995; Zhang et al. 1997; Mao et al. 1999; Williams et al. 2004). After blunders were eliminated, time series were analyzed using the *Create and Analyze Time Series* (*CATS*) package (Williams et al. 2004).

Jumps produced by CGPS stations configurations changes were corrected. Seasonal effects were also derived, by calculating annual and semiannual signals. Simultaneously, linear trends and offsets were obtained. Thus, it is feasible to identify the trend with the site linear velocity. Horizontal components in mm per year obtained at ROA are shown in Table SM5 (Supplementary Material).

### Analysis at the University of Jaen using Bernese and NEVE software

We processed independently with the same procedure two clusters of GPS data: one of them in the Iberian Peninsula from March 2008 to the end of 2012 and another one computed by the INGV in the European and Italian regions in the time span 1998–2012. This decision was taken in 2009 in order to obtain a set of fiducial stations which would be more stable due to the INGV time series being longer. The data analysis was performed with the Bernese Processing Engine (BPE) of the software Bernese 5.0, using the options shown in the Supplementary Material, Table SM3. A previous check of the quality of data was carried out using the TEQC software developed by UNAVCO (Estey and Meertens 1999).

We have estimated one daily solution in a loosely constrained reference frame, close to the rank deficiency condition. The output file is composed of the coordinates of the stations along with their covariance matrix in SINEX format. Loosely constrained solutions can be combined regardless of the datum definition of each contributing solution. The solution reference frame is defined stochastically by the input data and is basically unknown, but it is not necessary to estimate or to apply relative rigid transformations (rotation-translation scale) between reference frames and this naturally leads to a combined solution not distorted by any constrain or transformation. Therefore, our daily loosely constrained cluster solutions are then merged into global daily loosely constrained solutions of the whole network applying a classical least squares approach where the mathematical model is defined by the time propagation operator (Bianco et al. 2003). After that, the daily combined network solutions are minimally constrained and transformed into the ITRF2005 (Altamimi et al. 2007),

estimating translations and scale parameters. In particular, the realization EPN_A_ITRF2005 was used and 13 core stations contributed to the rigid transformation. These stations were AJAC, BOR1, BUCU, CAGL, EBRE, GRAS, GRAZ, LAMP, MATE, NOT1, SFER, SJDV and ZIMM.

We estimated the velocity field by using purposely designed software (NEVE) that manages the complete stochastic model (Devoti et al. 2008, 2011). Velocities were estimated simultaneously, together with annual signals and sporadic offsets at epochs of instrumental changes. The velocity field was estimated from ITRF2005 time series of daily coordinates with the complete covariance matrix. Velocity errors were derived from the direct propagation of the daily covariance matrix. Velocities for the horizontal components in mm per year obtained at UJA are shown in Annex II (Supplementary Material).

### Analysis at University of Barcelona (UB) using GAMIT/GLOBK

The University of Barcelona group (UB) analyzed data using GAMIT/GLOBK software (Herring et al. 2008) from the MIT that uses double differences of the phase and code data on the ionosphere-free (LC) combination to compute a network solution. We followed a three-step approach similar to the one described by McClusky et al. (2000). Previous to these steps, we performed a quality check of the analyzed stations, which included the examination of their monumentation, availability of the uninterrupted data, as well as the presence of correct information on the antenna and hardware changes in the provided log-files. In order to examine the quality of the actual GPS data given in daily *RINEX* files, we used the *TEQC* software from UNAVCO (Estey and Meertens 1999).

In the *first* step of our data analysis, we used daily GPS observations to estimate station coordinates together with estimates of the zenith delay of the atmosphere at each station. Orbital and Earth Orientation Parameters (EOP) were held fixed to the IGS final values by using a BASELINE mode. In the *second* step, we used these loosely constrained solutions to estimate consistent coordinates of the stations using the data combinations with the GLRED module of the GLOBK package. Afterward, we examined the time series of all the stations and removed obvious outliers following two criteria: if the position errors were higher than 20 mm and if the position itself was displaced more than 10 mm away from the best fitting trend line. Furthermore, some stations required offset corrections due to antenna changes. These steps were performed using several C-shell scripts specifically designed for this task, as well as, using interactive MATLAB® tools for viewing GPS velocities and time series developed by Herring

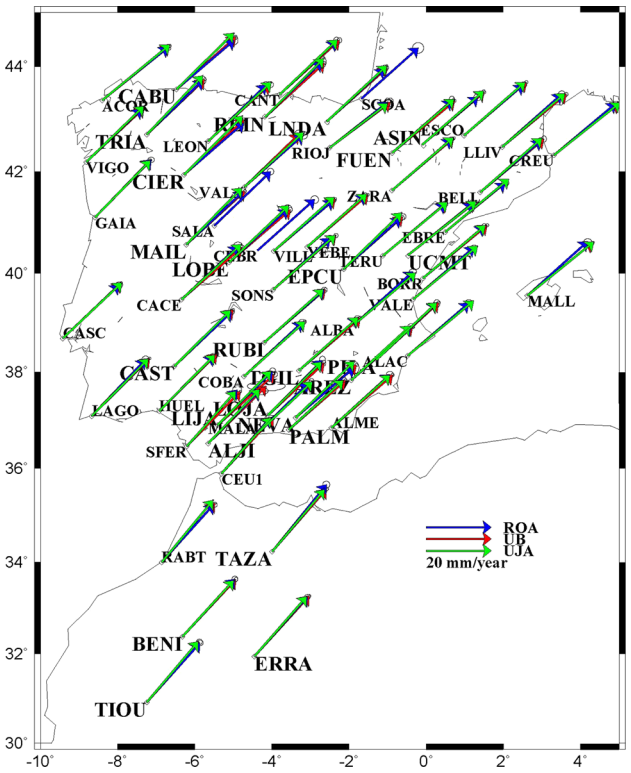


**Fig. 2** Topo-Iberia network velocities in the ITRF reference frame. The three different analysis groups derived these velocities from position time series. ROA (*blue*) and UB (*red*) solutions are in ITRF2008, while UJAEN (*green*) solution is in ITRF2005. As solutions are quite similar, some *arrows* seem to be hidden by the other analysis group results. *Values* can be found in Table SM5 (Supplementary Material)

(2003). Finally, the solution was realized in the ITRF2008 global reference frame (Altamimi et al. 2011), by minimizing the differences (using Helmert transformation) between our estimated horizontal velocities for the reference stations that have velocities computed in ITRF2008. The step of converting the ITRF2008 velocities into a Eurasia fixed reference frame is described in the next section. Figure 2 shows the results obtained for the three analysis groups in the International Terrestrial Reference Frame. Additional information can be found in the Supplementary Material: the detailed characteristics of the GAMIT/GLOBK processing performed by the UB are given in Table SM4, and the velocity field in ITRF2008 is displayed in Table SM5.

## Velocity solutions in the European Terrestrial Reference Frame (ETRF)

The ITRF velocity field maps are not well tuned to give an easy overview and interpretation of the tectonic behavior of the study area. Coordinates and velocities have to be

transformed to a regional reference frame to produce a velocity field, which may be understood more easily. This is done by applying a 14 parameter Helmert transformation. But this set of parameters should be derived also by including in our analysis points whose position and velocities are shown in the published Regional Reference Frame. In this analysis, we used a set of about 30 CGPS stations included in the European Permanent Networks and located in this region, so their position and velocities with respect to the European Terrestrial Reference Frame are well known. Using them as fiduciary points, the transformation parameters could be obtained. As an alternative method to use the calculated 14 parameters transformation, the ROA analysis group performed the seven parameters Helmert transformation on a daily basis, i.e., the transformation was applied to each individual daily solution for every analyzed station.

In this way, we obtained new time series that were analyzed with CATS software as well, in order to get the more accurate regional solution. Horizontal velocity components are shown in Table SM6 (Supplementary Material). All the site velocities are referred to the ETRF2000 reference frame. Those calculated at ROA are presented after CATS analysis, including again annual and semiannual seasonal signals, as well as the effects of the jumps over the time series.

The UJA group transformed the ITRF2005 solutions into the Eurasian Reference Frame using the Euler pole of the Eurasian plate published by Altamimi et al. (2007). Specifically, the Euler pole parameters employed were: 56.33°N, 95.98°W and 0.261 ± 0.003°/Myr.

The UB group resorted to a somewhat different approach in order to estimate the Eurasia fixed reference frame. They estimated the Euler pole of the Eurasian plate and transformed the ITRF2008 solutions into the Eurasian Reference Frame. To calculate the Euler Pole, different groups of reference CGPS stations defining the Eurasian Reference Frame were used. As a selection criterion, we chose the maximum horizontal residual velocity of 0.3 mm/year, which provided us with a set of ten sites that define a fixed Eurasia.

However, since the three analysis groups used somewhat different procedures to transform the ITRF velocities to the ETRF reference frame, we performed the unification of the 3 velocity solutions, as described below.

## Combination

To ensure the consistency between the three estimates of the velocities by the group, we transformed the ITRF each group solution to a common Eurasia Reference Frame determined using the three Cartesian components

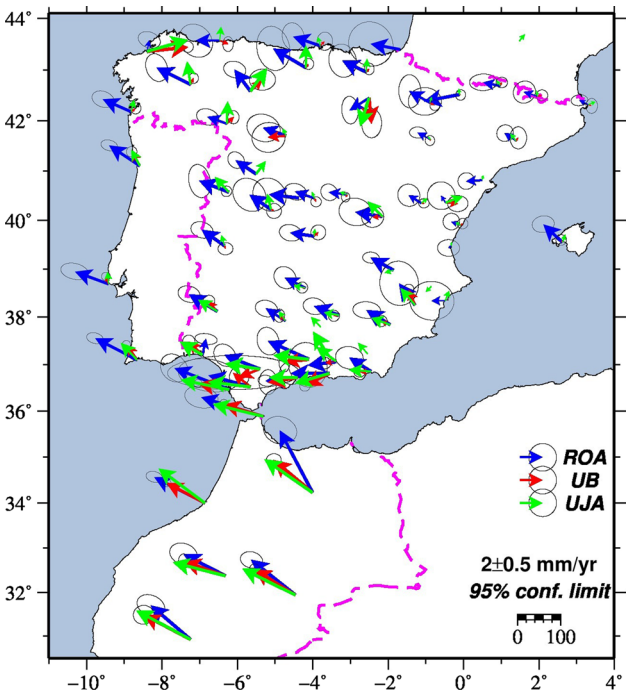


**Fig. 3** ETRF2000 velocities derived from position time series produced by GIPSY–OASIS software after time series analysis with CATS (*blue arrows*); GAMIT/GLOBAK at UB (*red arrows*); and Bernese and NEVE at UJA (*green arrows*). *Error ellipses* denote 95 % confidence intervals

of the Eurasia Euler pole (wx = −0.021890; wy = −0.147500; wz = 0.213100 in deg/Myr), as defined by the ITRF2008 (Altamini et al. 2011). The transformation was performed using the VELROT V1.01 velocity field comparison and combination software included in the GLOBK/GAMIT analysis package (Herring et al. 2008). After a 6-parameter transformation (translational and rotation), we obtained the three consistent solutions in the Eurasia fixed ITRF2008 frame for the 25 Topo-Iberia stations (Fig. 4a).

After the combination procedure was performed, the velocities estimated by the three groups were considerably more consistent with each other. For example, a northward motion observed in the UJA estimated velocities for the stations CABU, REIN and LNDA (green vectors in Fig. 3) is not visible any more.

We also used the VELROT program to calculate an average velocity field from the three solutions for the 25 stations of the Topo-Iberia network. These results are shown in Table 1 and in the bottom panel of Fig. 4, but also in GMT format in Table SM7 (Supplementary Material). Results for the other CGPS stations in the area but also for the EUREF stations fixed to make the transformation from the ITRF to the ETRF are shown in Table SM8 (Supplementary Material).

**Table 1** Topo-Iberia GPS network combined velocities (mm/year) with their standard deviations in the ETRF Frame

| # | STA ID | East ± 1σ | North ± 1σ |
|---|---|---|---|
| 1 | ALJI | −3.45 ± 0.10 | 0.05 ± 0.09 |
| 2 | AREZ | −1.56 ± 0.06 | 0.26 ± 0.07 |
| 3 | ASIN | −0.27 ± 0.12 | −0.04 ± 0.13 |
| 4 | BENI | −4.08 ± 0.10 | 0.96 ± 0.11 |
| 5 | CABU | 0.17 ± 0.08 | 0.25 ± 0.10 |
| 6 | CAST | −1.41 ± 0.06 | 0.53 ± 0.07 |
| 7 | CIER | 0.18 ± 0.07 | 1.02 ± 0.08 |
| 8 | EPCU | −1.32 ± 0.08 | 0.64 ± 0.08 |
| 9 | ERRA | −4.19 ± 0.11 | 2.19 ± 0.11 |
| 10 | FUEN | 0.02 ± 0.10 | −0.14 ± 0.11 |
| 11 | LIJA | −2.73 ± 0.07 | −0.04 ± 0.08 |
| 12 | LNDA | −0.04 ± 0.10 | 0.36 ± 0.12 |
| 13 | LOBE | −0.21 ± 0.07 | 0.63 ± 0.07 |
| 14 | LOJA | −2.87 ± 0.06 | −0.08 ± 0.07 |
| 15 | MAIL | −0.98 ± 0.07 | 0.56 ± 0.07 |
| 16 | NEVA | −1.51 ± 0.08 | 0.48 ± 0.09 |
| 17 | PALM | −2.79 ± 0.07 | −1.23 ± 0.07 |
| 18 | PILA | −1.19 ± 0.06 | 1.16 ± 0.07 |
| 19 | REIN | −0.10 ± 0.08 | 0.96 ± 0.10 |
| 20 | RUBI | −0.86 ± 0.06 | −0.23 ± 0.06 |
| 21 | TAZA | −3.87 ± 0.15 | 2.96 ± 0.15 |
| 22 | TGIL | −1.17 ± 0.06 | −0.18 ± 0.07 |
| 23 | TIOU | −4.12 ± 0.13 | 2.28 ± 0.13 |
| 24 | TRIA | −0.23 ± 0.07 | 1.07 ± 0.07 |
| 25 | UCMT | 1.20 ± 0.12 | 0.04 ± 0.11 |

ASCII format file to be used in GMT psvelo routine is provided as a supplementary material

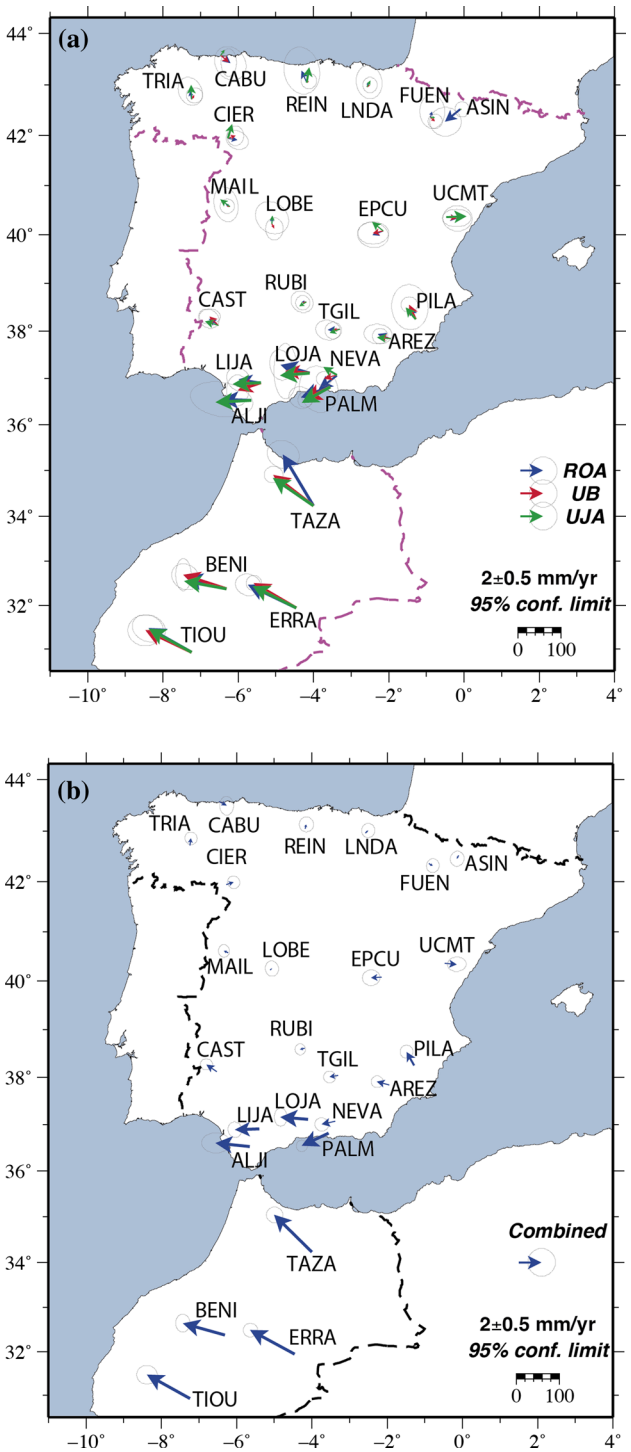


**Fig. 4** **a** (*Top panel*): Eurasia fixed velocities derived from VELROT transformations. ROA: (*blue*); UB (*red*); UJA (*green*). **b** (*Bottom panel*): Average velocity field of the Topo-Iberia GPS network in Eurasia fixed ITRF2008. This was obtained from the combination of the three solutions from ROA, UB and UJA. *Error ellipses* denote 95 % confidence intervals

## Discussion

Starting in the Pyrenees mountain belt in the north, which separates the Iberian Peninsula from the rest of the European continent, and going to the south, the majority of the observed points show very small velocity residuals with respect to the ETRF. However, in the southernmost part of the Iberian Peninsula, the residual motions become more prominent. This is not surprising, since this part includes a plate boundary zone that accommodates approximately 5 mm/year relative motion between the Eurasian and Nubian tectonic plates (McClusky et al. 2003). The largest velocities are observed for the stations located in Morocco, since these points are not located on the Eurasian plate but instead belong to the Nubian tectonic plate.

### Strain rate calculation

Strain rate parameters were calculated for all the processed stations within the study area: Iberia and North Africa. However, since the spatial coverage of the stations in North Africa was limited (only 6 stations were processed), the statistically significant results were only obtained for the region on the Iberian Peninsula and the Alboran sea. The

strain rate field calculation was performed using the SSPX software package (Cardozo and Allmendinger 2009). We used the grid-nearest neighbor approach that computes strain rate at the center of each square, with a grid spacing of 70 km and the 7 nearest stations located within a maximum distance of 200 km. These parameters provide a smoothed regional pattern, and some local strain field variations could have been missed. The horizontal principal strain rate axes and dilatation are shown in Fig. 5a. Figure 5b shows maximum shear strain rates and the direction of left-lateral motion. The right-lateral motion would be oriented perpendicular to the shown direction. In all cases, only statistically significant values at $1\sigma$ level are presented. Positive dilatational strain rates in Fig. 5a, shown in red colors, indicate extension, while negative values, shown in blue, indicate compression.

Maximum deformation signal is observed in the Central Betics and northern Alboran Sea. Here both the dilatation and the shear strain rates reach their maximum values: WSW-ENE extension of approximately 30 nstrain/year (Fig. 5a) and shear strain rate (Fig. 5b) of 25 nstrain/year oriented approximately WSE-NNW for the left-lateral shear (green axis). The Central Betic zone is known for its high rate of seismicity. In 1910, an $M_w$6.1 earthquake occurred near the city of Adra, which had an oblique-strike-slip focal mechanism (Stich et al. 2003), roughly in agreement with the strain rate direction estimated from the GPS velocities. Moreover, previous geodetic studies showed that the Balanegra fault, located just east of Adra, exhibits an uplift rate between 0.09 and 0.12 mm/year, indicating a horizontal WSW-ESE regional extension (Marín-Lechado et al. 2010).

A small region of high shear strain rate is observed in the east-central part of the peninsula, near Alicante. This highly deforming zone is most likely related to the Crevillente (or Cadiz-Alicante) fault system, which causes a westward displacement of the Betic Internal Zone and part of the External Zone (e.g., Sanz de Galdeano and Buforn 2005). Part of the strain can be attributed to the Alhama de Murcia fault (Echeverria et al. 2013), responsible for the $M_w$5.2 11/05/2011 Lorca earthquake (Frontera et al. 2012; Martínez-Díaz et al. 2012). However, with the given spatial coverage, it might be a bit hasty to unambiguously attribute the observed shear strain rates to the Crevillente fault system.

Strain rate calculations are also in agreement with Pérez-Peña et al. (2010), although they used Delaunay triangulation to calculate the strain rates. Similarly, our results agree with those presented by Fadil et al. (2006), although their deformation rates are somewhat higher and located farther to the south in the Alboran Sea, probably due to the utilization of a denser data set from Morocco.

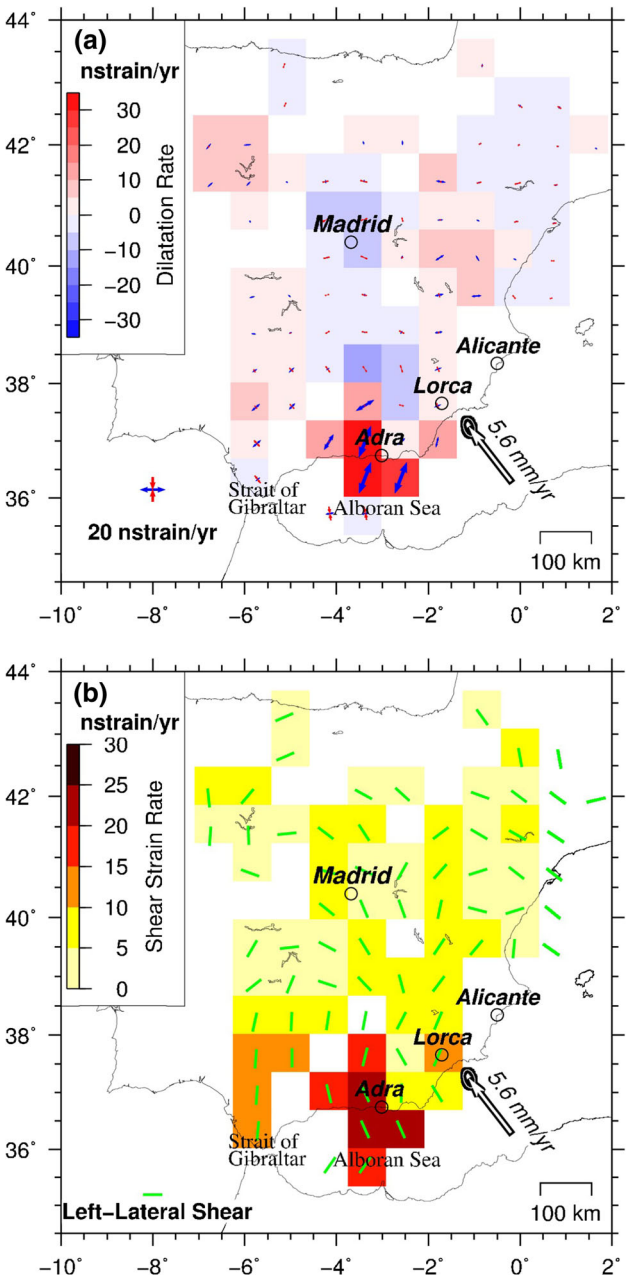


**Fig. 5** GPS strain rate field computed for the Iberian Peninsula. *Double arrow* to the right shows Nubia-Eurasia plate convergence velocity based on NNR-MORVEL56 model (Argus et al. 2011). **a** (*Top panel*): 2D dilatation strain rates: *blue* is compression; *red* is extension. The *blue axis* indicates a direction of extension and the *red axis* a direction of compression; **b** (*Bottom panel*): Maximum shear strain rates. The *color scale* indicates the magnitude of the maximum shear strain rate. *Green lines* in the middle of the grid indicate the maximum sinistral shear directions

Minor deformation rates can be observed around the Strait of Gibraltar and the Gulf of Cadiz (blue boxes in Fig. 5a). Here we observe negative dilatation rates (i.e., compression) of 4 nstrain/year indicating a compression oriented toward WNW-ESE, in agreement with the

orientation of the maximum contractional-horizontal strain rate estimated by Palano et al. (2013).

When talking about strain rates, we found a maximum strain rate offshore at the Alboran Sea to the south of the Betics. Another maximum was found close to the Gulf of Cadiz. This pattern is quite similar to the strain rates of Palano et al. (2013), although the magnitudes are slightly different. As expected, the estimated strain rates decrease to the north, where the deformation rates are smaller.

## Conclusions

In the framework of the Topo-Iberia project, we established a geodetic network of 21 continually operating GPS stations in Spain and 4 in Morocco. Considerable financial and human resources were dedicated to a correct design and monumentation of the network, which took the first 2 years of the project. Since the main goal behind the establishment of the Topo-Iberia GPS network was the detection of relatively slow (<5 mm/year) tectonic deformations throughout the Iberian Peninsula and northern Africa, we ensured the geodetic monuments were stable and the detected velocities were indeed related to the long-term geologic and tectonic motions.

More specifically, through an increased spatial coverage of the CGPS stations and state-of-the-art analysis procedure, we have been able to provide a contemporary crustal deformation velocity field for the Iberian Peninsula and Morocco with an unprecedented precision. Maximum horizontal velocities in the Eurasia frame are observed for the stations located on the Africa (i.e., Nubia) tectonic plate in Morocco, where the calculated velocities range from 4.2 to 4.9 mm/year (Fig. 4; Table 1). Within the Iberian Peninsula, maximum velocities are observed in the southern margin, close to the Strait of Gibraltar and the Betics. Here the velocities reach 3.5 mm/year at ALJI, indicating that the tectonic behavior of this region is influenced more by the African plate than the Eurasian. The estimated $1\sigma$ uncertainties for the calculated velocities are low, below 0.2 mm/year.

To conclude, the main achievements of the Topo-Iberia GPS project can be considered the establishment of the highly stable CGPS network in Spain and Morocco. Currently, we are in the process of incorporating this network into the European Plate Observing System (EPOS), an integrated solid earth sciences research infrastructure included in the ESFRI Roadmap in December 2008 (www.epos-eu.org). As a result, we hope that the entire Topo-Iberia network will continue operating. Data will become available to a wide range of users, not limited to scientists studying earthquakes and tectonics, but will include practitioners of geodesy and climate research.

**Acknowledgments** This research has been funded by the Spanish Government through the research project "Geosciences in Iberia: Integrated studies on topography and 4-D evolution" (CSD2006-00041). We acknowledge all those people, representing various institutions, who participated in searching for appropriate site locations, and their consequent installation and operation. Also, we would like to thank the landowners who gave their generous permission to install the scientific equipment on their properties. Most of the figures were prepared using the public domain Generic Mapping Tools GMT (Wessel et al. 2013).

## References

Altamimi Z, Collilieux X, Legrand J et al (2007) ITRF2005: a new release of the international terrestrial reference frame based on time series of station positions and earth orientation parameters. J Geophys Res 112:B09401. doi:10.1029/2007JB004949

Altamimi Z, Collilieux X, Métivier L (2011) ITRF2008: an improved solution of the international terrestrial reference frame. J Geod 85:457–473. doi:10.1007/s00190-011-0444-4

Argus DF, Gordon RG, DeMets C (2011) Geologically current motion of 56 plates relative to the no-net-rotation reference frame. Geochem Geophys Geosystems 12:Q11001. doi:10.1029/2011GC003751

Avallone A, Selvaggi G, D'Anastasio E et al (2010) The RING network: improvement of a GPS velocity field in the central Mediterranean. Ann Geophys 53:39–54. doi:10.4401/ag-4549

Bianco G, Devoti R, Luceri V (2003) Combination of loosely constrained solutions. In: Richter B, Schwegmann W, Dick WR (eds) Proceedings of the IERS workshop on combination research and global geophysical fluids, pp 107–109

Blewitt G, Lavallée D (2002) Effect of annual signals on geodetic velocity. J Geophys Res 107:1–9. doi:10.1029/2001JB000570

Bruyninx C, Altamimi Z, Boucher C et al (2009) The European reference frame: maintenance and products. In: Drewes H (ed) Geodetic reference frames. Springer, Berlin, pp 131–136

Cardozo N, Allmendinger RWW (2009) SSPX: a program to compute strain from displacement/velocity data. Comput Geosci 35:1343–1357. doi:10.1016/j.cageo.2008.05.008

Dach R, Hugentobler U, Fridez P, Meindl M (2007) Bernese GPS software version 5.0. User manual. Astron Institute, Univ Bern, vol 640, p 640

Devoti R, Riguzzi F, Cuffaro M, Doglioni C (2008) New GPS constraints on the kinematics of the Apennines subduction. Earth Planet Sci Lett 273:163–174. doi:10.1016/j.epsl.2008.06.031

Devoti R, Esposito A, Pietrantonio G et al (2011) Evidence of large scale deformation patterns from GPS data in the Italian subduction boundary. Earth Planet Sci Lett 311:230–241. doi:10.1016/j.epsl.2011.09.034

Dietrich R, Dach R, Engelhardt G et al (2001) ITRF coordinates and plate velocities from repeated GPS campaigns in Antarctica—an analysis based on different individual solutions. J Geod 74:756–766. doi:10.1007/s001900000147

Echeverria A, Khazaradze G, Asensio E et al (2013) Crustal deformation in eastern Betics from CuaTeNeo GPS network. Tectonophysics 608:600–612. doi:10.1016/j.tecto.2013.08.020

Estey LH, Meertens CM (1999) TEQC: the multi-purpose toolkit for GPS/GLONASS data. GPS Solut 3:42–49

Fadil A, Vernant P, McClusky S et al (2006) Active tectonics of the western Mediterranean: geodetic evidence for rollback of a delaminated subcontinental lithospheric slab beneath the Rif Mountains, Morocco. Geology 34:529–532. doi:10.1130/G22291.1

Frontera T, Concha A, Blanco P et al (2012) DInSAR coseismic deformation of the May 2011 Mw 5.1 Lorca earthquake (southeastern Spain). Solid Earth 3:111–119. doi:10.5194/se-3-111-2012

Herring T (2003) MATLAB tools for viewing GPS velocities and time series. GPS Solut 7:194–199. doi:10.1007/s10291-003-0068-0

Herring TA, King RW, McClusky SC (2008) Introduction to GAMIT/GLOBK. Massachusetts Institute of Technology, Cambridge

Johnson HO, Agnew DC (1995) Monument motion and measurements of crustal velocities. Geophys Res Lett 22:2905–2908. doi:10.1029/95GL02661

Kierulf HP, Plag HP, Bingley RM et al (2008) Comparison of GPS analysis strategies for high-accuracy vertical land motion. Phys Chem Earth 33:194–204. doi:10.1016/j.pce.2006.11.003

Mao A, Harrison CGA, Dixon TH (1999) Noise in GPS coordinate time series. J Geophys Res 104:2797. doi:10.1029/1998JB900033

Marín-Lechado C, Galindo-Zaldívar J, Gil AJ et al (2010) Levelling profiles and a GPS network to monitor the active folding and faulting deformation in the Campo de Dalias (Betic Cordillera, Southeastern Spain). Sensors 10:3504–3518. doi:10.3390/s100403504

Martínez-Díaz JJ, Bejar-Pizarro M, Álvarez-Gómez JA et al (2012) Tectonic and seismic implications of an intersegment rupture. Tectonophysics 546–547:28–37. doi:10.1016/j.tecto.2012.04.010

McClusky S, Balassanian S, Barka A et al (2000) Global positioning system constraints on plate kinematics and dynamics in the eastern Mediterranean and Caucasus. J Geophys Res 105:5695–5719. doi:10.1029/1999JB900351

McClusky S, Reilinger R, Mahmoud S et al (2003) GPS constraints on Africa (Nubia) and Arabia plate motions. Geophys J Int 155:126–138. doi:10.1046/j.1365-246X.2003.02023.x

Palano M, González PJ, Fernández J (2013) Strain and stress fields along the Gibraltar Orogenic Arc: constraints on active geodynamics. Gondwana Res 23:1071–1088. doi:10.1016/j.gr.2012.05.021

Pérez-Peña A, Martín-Davila J, Gárate J et al (2010) Velocity field and tectonic strain in southern Spain and surrounding areas derived from GPS episodic measurements. J Geodyn 49:232–240. doi:10.1016/j.jog.2010.01.015

Sanz de Galdeano C, Buforn E (2005) From strike-slip to reverse reactivation: the Crevillente fault system and seismicity in the Bullas-Mula area (Betic Cordillera, SE Spain). Geol Acta 3:241–250

Scherneck H-G (1991) A parametrized solid earth tide model and ocean tide loading effects for global geodetic baseline measurements. Geophys J Int 106:677–694. doi:10.1111/j.1365-246X.1991.tb06339.x

Stich D, Batllo J, Morales J et al (2003) Source parameters of the MW=6.1 1910 Adra earthquake (southern Spain). Geophys J Int 155:539–546. doi:10.1046/j.1365-246X.2003.02059.x

Wessel P, Smith WHF, Scharroo R et al (2013) Generic mapping tools: improved version released. EOS Trans Am Geophys Union 94:409–410. doi:10.1002/2013EO450001

Williams SDP, Bock Y, Fang P et al (2004) Error analysis of continuous GPS position time series. J Geophys Res 109:B03412. doi:10.1029/2003JB002741

Zhang J, Bock Y, Johnson H et al (1997) Southern California permanent GPS geodetic array: error analysis of daily position estimates and site velocities. J Geophys Res 102:18035. doi:10.1029/97JB01380

Zumberge JF, Heflin MB, Jefferson DC et al (1997) Precise point positioning for the efficient and robust analysis of GPS data from large networks. J Geophys Res 102:5005. doi:10.1029/96JB03860

**Jorge Garate** is Head of Satellite Service at San Fernando Naval Observatory (ROA) since 1993. He is the GNSS research activities responsible and manager of the Satellite Laser Ranging Station at ROA. He has a Science PhD for the University of Cadiz (2000), and a B.Sc. (Physics) for the University of Zaragoza (1992).

**Giorgi Khazaradze** is an Associate Professor at the faculty of Geology at the University of Barcelona. His research focuses on tectonic applications of space geodesy. He earned his PhD (Geophysics) from the University of Washington (1999) and B.E. (Engineering Geophysics) from Tbilisi State University (Georgia) in 1990.

**M. Clara de Lacy** is an associate professor of Geodesy at the department of Cartographic, Geodetic and Photogrammetric Engineering in the University of Jaen. She is member of the UJA Geodesy Research Group. She is involved in research on GNSS positioning and navigation using GPS and Galileo, crustal deformation monitoring and engineering geodesy.